32nd URSI GASS, Montreal, 19-26 August 2017

# Accurate geolocation of RFI sources from SMOS interferometric data

Eric Anterrieu, Ali Khazaal, François Cabot and Yann Kerr
CESBIO, Université de Toulouse, CNRS, CNES & IRD
13 avenue Colonel Roche, 31400 Toulouse, France

## Abstract

The SMOS mission is a European Space Agency project aimed at global monitoring of surface Soil Moisture and Ocean Salinity from radiometric L-band observations. Although the L-band is a protected band, the data collected by SMOS are contaminated by radio frequency interferences (RFI) which degrade the performance of the mission. A precise location of the RFI emitters is required for switching-off illegal transmissions or for fixing malfunctioning equipments. This work is concerned with the geolocation of such sources with a sub-kilometric accuracy from SMOS interferometric data themselves.

## 1. Introduction

MIRAS (Microwave Imaging Radiometer by Aperture Synthesis) is the single payload of the SMOS (Soil Moisture and Ocean Salinity) space mission led by the European Space Agency and launched in November 2009. MIRAS is a Y-shaped interferometric array fitted with 69 equally spaced antennas operating in the L-band. The signals collected by each pair of antennas are cross-correlated and provide samples of the so-called visibility function of the brightness temperature distribution of the scene under observation. Visibility samples are inverted with the aid of the computer in a regularized reconstruction procedure which aims at retrieving the brightness temperature distribution [1].

Although MIRAS is operating in a protected band, the contamination of these measurements by man-made sources of radio-frequency interferences (RFIs) operating very close to the L-band has been expected [2] and is frequently observed [3]. Although the geolocation of such RFI sources has already been addressed, the accuracy is almost always kilometric (≥ 1 Km) [4]. This contribution is devoted to a major improvement recently brought to this problem by introducing an approach that performs the geolocation of such RFI sources with a sub-kilometric accuracy (< 1 Km) [5]. Such performances are illustrated with the aid of numerical simulations as well as with real data acquired by MIRAS interferometer.

## 2. Parametric approach

RFI sources are modeled according to a parametric model where the location and the brightness temperature of the source at ground level are the key parameters. These parameters are optimized in a constrained iterative process where the visibilities corresponding to a given RFI source are computed with the actual modeling of the instrument and subtracted from the visibilities acquired by MIRAS. With regards to the location, two approaches have been studied. In a first approach, each snapshot is processed independently. Since there is no guarantee that a given RFI source is found at the same ground location in all the snapshots, the average or the median location is retained. In a second approach, the same snapshots are processed all together so that for any RFI source there is by definition a unique ground location for the group. However, the drawback of this approach is a larger computational time compare to the previous one. Moreover, this global approach precludes any post-processing such like the filtering of outliers which may have a strong impact on the final location. As a consequence, the first approach is clearly encouraged.

Complex visibilities have been simulated for many scenes over Spain corrupted by a RFI source located in Madrid. Shown in Figure 1 in the reference frame of MIRAS is one of these many reconstructed snapshots when inverting these simulated visibilities. The stronger effects of the RFI source are visible close to the source with high resolution oscillations.

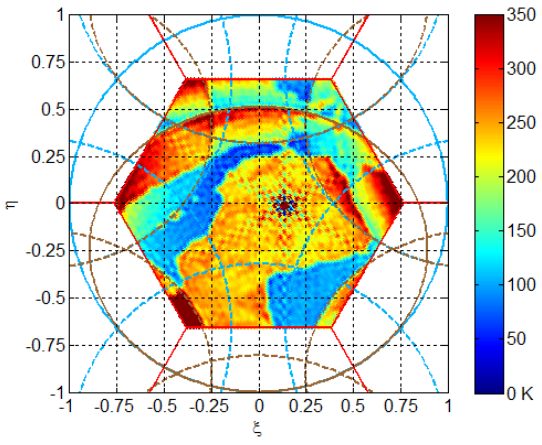


**Figure 1.** Brightness temperature distribution of a reconstructed snapshot in the reference frame of MIRAS: the effects of an RFI source over Madrid are clearly visible.

As shown in Figure 2, the local mean $\mu_\ell$ around an RFI source is highly impacted by the presence of the source. This is not the case of the local standard deviation $\sigma_\ell$. The idea is therefore to minimize $\sigma_\ell$ in the vicinity of the RFI source where the oscillating effects of the RFI source are stronger. Since high resolution features are looked for, $\sigma_\ell$ has to be computed at the highest level of resolution achievable by the instrument, namely without any apodization. The variations of the local standard deviation shown in Figure 2 suggest to compute $\sigma_\ell$ in a disk of radius $\rho \approx 0.03$ centered on the closest pixel to the RFI source because it exhibits a bump around this value.

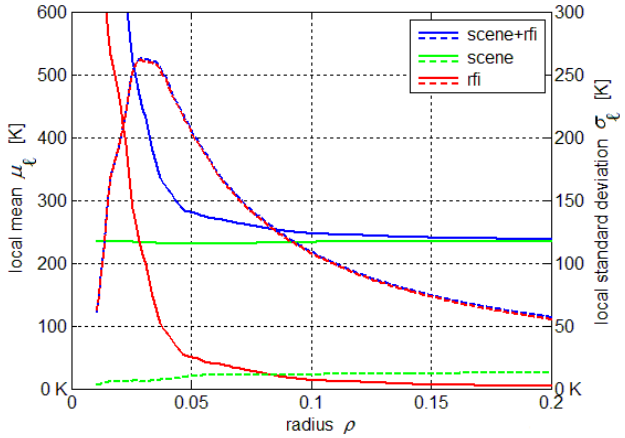


**Figure 2.** Variations of the local mean (solid lines) and of the standard deviation (dashed lines) of the brightness temperature in disks of growing radii centered on the RFI source.

According to the optimizations performed with these simulated visibilities, the ground location of the RFI source can be achieved with a sub-kilometric accuracy. However, this has to be confirmed with real SMOS data.

## 3. Illustrations and results

Among the many RFI sources affecting SMOS data worldwide, few of them have been geolocated, especially in Europe. For most of them, ground coordinates have been provided by authorities of the corresponding country but without the possibility to check them. However, for a very small number, these coordinates have been cross-checked with independent GPS measurements and/or accompanied with a ground truth.

This is the case of a RFI emitter geolocated in Ukraine with GPS coordinates 48°6′17.00″ N and 33°32′13.40″ E. Shown in Figure 3 are the 13 orbits passing close to this emitter in June 2011. More than 1100 snapshots having this point in the alias-free field of view of SMOS have been processed in X and Y polarizations. Ascending and descending passes have been treated separately.

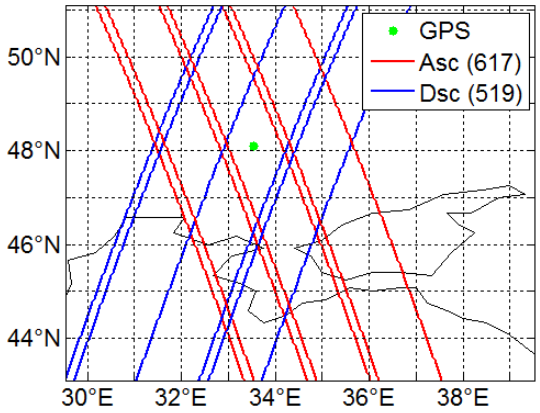


**Figure 3.** Ascending (red) and descending (blue) orbits passing close to the RFI source in Ukraine (green dot) during June 2011.

Shown in Figure 4 are the raw estimations of the locations of the source. The orientation of the 95% confidence ellipses centered on the average locations of the distributions are comparable to the footprint's local orientation of the ascending and descending orbits at the latitude of this RFI source. However, as expected, they do not share the same center and consequently ascending and descending passes do not lead to the same ground coordinates. The estimate obtained with 617 snapshots from the 7 ascending orbits, 48°6′14.21″ N and 33°32′5.44″ E, is about 185 m westward from the GPS coordinates of the source whereas the estimate obtained with 519 snapshots from the 6 descending orbits, 48°6′21.01″ N and 33°32′33.00″ E, is about 420 m eastward from the GPS coordinates of the source. These two estimates are more than 600 m distant from one another.

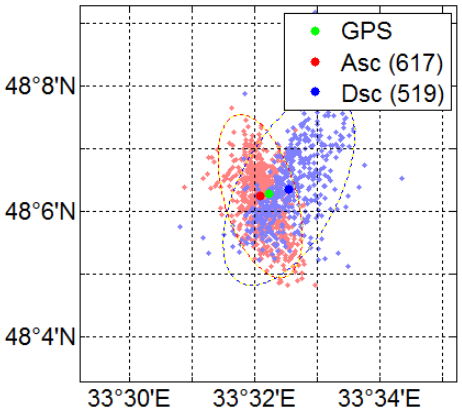


**Figure 4.** Raw estimations of the locations (light red and light blue dots) of the RFI source in Ukraine: the final estimations (dark red and dark blue dots) are not sharing the same ground location.

A unique estimate can be obtained by computing the average of the two previous ones: 48°6′17.61″ N and 33°32′19.22″ E, which is only 120 m from the GPS coordinates of the source. However, another approach is preferred. Owing to the locations of the ascending and descending estimates with regards to the GPS coordinates of the source, a certain amount of the observed difference can be attributed to a bias due to a potential mispointing of the platform. This bias can be reduced by computing the yaw, pitch and roll angles that make the estimates from ascending and descending passes one single point. The values of the Cardan angles that realize this non-linear optimization are: +0.88″ (yaw), −1.02″ (pitch) and +0.60″ (roll). The corresponding optimized estimations of the locations of the source obtained are shown in Figure 5. The unique estimate thus obtained, 48°6′20.11″ N and 33°32′17.19″ E, is now less than 125 m from the GPS coordinates of the source. These coordinates slightly differ from the previous average ones, but they are more consistent with the attitude of the platform.

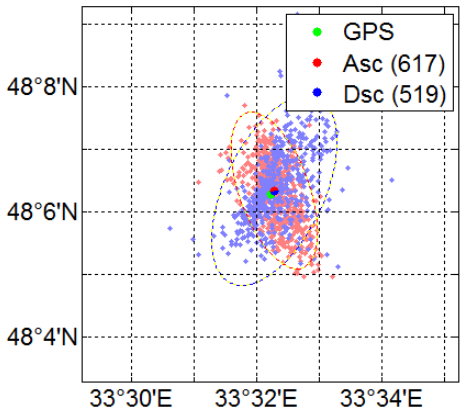


**Figure 5.** Optimized estimations of the locations (light red and light blue dots) of the RFI source in Ukraine: the final estimations (dark red and dark blue dots) are now sharing the same ground location.

Coming back to the objective of the method which is to provide an accurate estimation of the location of RFI emitters, the region of uncertainty is naturally defined here by the intersection of the ascending and descending 95% uncertainty confidence ellipsis, both being centered on the final estimation of the location. It is important to keep in mind that the area of this uncertainty region can only be reduced by increasing the number of snapshots processed.

Very similar results have been obtained over other months with about the same number of snapshots processed. As mentioned in Table I of [4], the ground distance between the true location of the same RFI source (named UA 1) and the estimation provided by the authors of that study is 2.35 Km.

The same processing has been performed with another RFI source over Germany. More than 800 snapshots have been processed but over a longer period of time (6 months) because this RFI source turned out to be frequently switched off which arithmetically reduces the number of snapshots to process. As a consequence, the final accuracy on the location of this RFI source is here about 160 m, still sub-kilometric. This source also appears in Table I of [4] (under the name DE 1) and the accuracy of its geolocation announced by the authors of that study is 4.00 Km.

As shown in Figure 6, only a sub-kilometric geolocation allows the ground identification of an RFI source from high-resolution close views of the region from space (like those provided by GoogleMaps, for example).

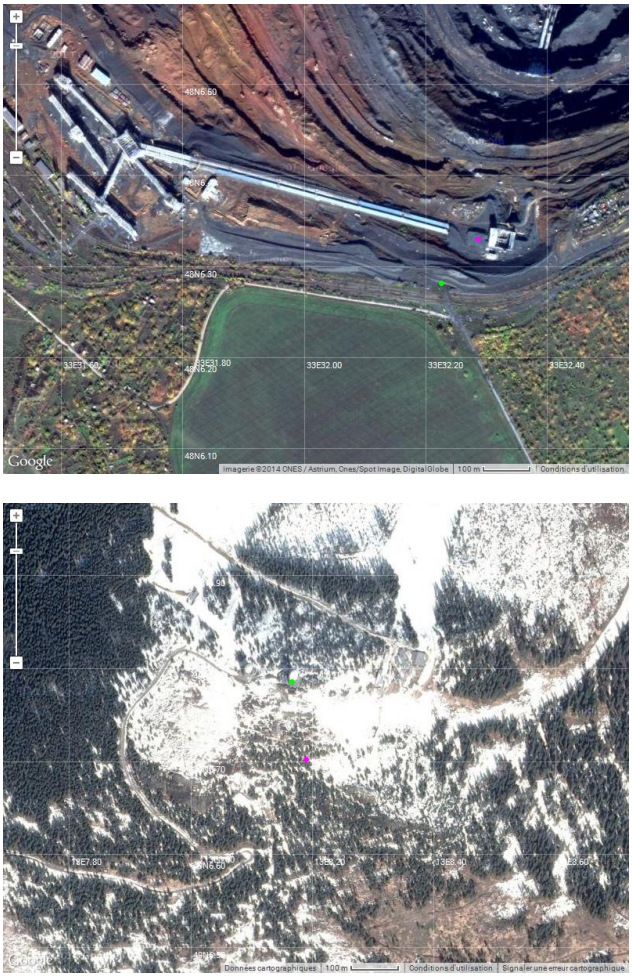


**Figure 6.** Google maps high-resolution close views over Ukraine (on the top) and over Germany (on the bottom) with the true location of the RFI sources (green dot) and their final estimations (purple dot).

## 4. Conclusion

Obviously, many RFI sources are still emitting in the protected L-band all around the world and unfortunately

they are contaminating SMOS measurements. Based on these encouraging results obtained on a limited number of sources, the systematic geolocation of some of them has started. It is a huge task since the number of snapshots to process is large and the method is time consuming. The main bottleneck is the selection of the snapshots which is not actually fully automatic but is dimensioning with respect to the accuracy of the final result. Nevertheless, with an accuracy well below 1000 m one can quickly provide sufficient evidence as to the position of the emitter and enable fast action from the national spectrum management agencies.

## 4. References


[1] E. Anterrieu and A. Khazaal, "Brightness temperature maps reconstruction from dual-polarimetric visibilities in synthetic aperture imaging radiometry," IEEE Transactions on Geoscience and Remote Sensing, 46(3), pp. 606-612, Mar. 2008.

[2] A. Camps, I. Corbella, F. Torres, J. Bara and J. Capdevila, "RF interference analysis in aperture synthesis interferometric radiometers: application to L-band MIRAS instrument," IEEE Transactions on Geoscience and Remote Sensing, 38(2), pp. 942-950, Mar. 2000.

[3] R. Oliva, E. Daganzo-Eusebio, Y.H. Kerr, S. Mecklenburg, S. Nieto, P. Richaume and C. Gruhier, "SMOS radio frequency interference scenario: status and actions taken to improve the RFI environment in the 1400–1427-MHz passive band," IEEE Transactions on Geoscience and Remote Sensing, 50(5), pp. 1427-1439, May. 2012.

[4] R. Oliva, S. Nieto and F. Félix-Redondo, "RFI detection algorithm: accurate geolocation of the interfering sources in SMOS images," IEEE Transactions on Geoscience and Remote Sensing, 51(10), pp. 4993-4998, Oct. 2013.

[5] E. Anterrieu, A. Khazaal, F. Cabot and Y.H. Kerr, "Geolocation of RFI sources with sub-kilometric accuracy from SMOS interferometric data," Remote Sensing of Environment, 180, pp. 76-84, Jul. 2016.